

## Damping Mechanism in Dynamic Force Microscopy

Michel Gauthier and Masaru Tsukada

*Department of Physics, Graduate School of Science, University of Tokyo, Hongo 7-3-1, Bunkyo-ku, Tokyo 113-0033, Japan*  
(Received 12 July 2000)

A general theory is presented which describes the damping in dynamic force microscopy due to the proximity of the surface, consistently with resonant frequency shift effects. Orders of magnitude for the experimentally measured “dissipation” and image corrugation are reproduced. It is suggested that the damping does not mainly result from energy dissipation, but arises because not all solutions of the microlever equation of motion are accessible. The damping is related to the multivalued nature of the analytical resonance curve, which appears at some critical tip-surface separation.

PACS numbers: 61.16.Ch, 07.79.Lh, 87.64.Dz

Dynamic force microscopy (DFM) is a versatile tool that is now currently used for studying conducting as well as insulating surfaces. The basic experimental setup was mainly designed by Albrecht *et al.* [1] where a microlever is used as a resonator for sensing the interaction between the tip attached to it and the surface. The experimental demonstration of its usefulness for imaging surfaces at an atomic scale [2–4] in ultrahigh vacuum has attracted considerable interest. Despite these impressive technical advances, the physics underlying its atomic resolution capability, the imaging contrast in particular, is still not clearly elucidated. The problem appears to be twofold. On the one hand, the forces involved greatly depend on the chemical nature of the sample and tip (sometimes contaminated by sample atoms) and also on the shape of the tip so that a definite and general conclusion is rather difficult to draw. Besides, the physical meaning of experimentally measured quantities used for imaging is not always straightforward to interpret. For instance, while the shift of the microlever resonant frequency is generally accepted to represent some average of the interaction force [5], the situation is quite alarming regarding the damping of the lever due to the proximity of the surface [6–9]. Various mechanisms by which the lever energy may be dissipated have been suggested [6,9–11] depending on the strength and nature of the interaction, and also on mechanical properties of the surface. Despite this, convincing quantitative approaches capable of reproducing *even* orders of magnitude of experimentally inferred dissipation have not been presented yet, presumably indicating that the nature of the damping in DFM has so far proved elusive.

It may be important to draw a distinction between the damping and dissipation mechanisms involved in DFM. While any energy transfer from the tip to the surface would obviously result in a reduction of the lever oscillation amplitude, the existence of damping may not necessarily imply that some dissipative process is involved. First, in constant amplitude experiments, the energy dissipation is not directly assessed but inferred by measuring the change of the driving signal amplitude  $\Delta A_d \equiv A_d - A/Q_0$  (a measure of the damping) or equivalently the quality fac-

tor  $Q \equiv A/A_d$  through the relation  $\Delta E = kA/2\Delta A_d = kA^2/2(1/Q - 1/Q_0)$ , where  $k$  is the lever spring constant and  $A/Q_0$  the driving amplitude necessary in order to compensate for the intrinsic dissipation. Second, because the interaction energy is much smaller than that of the lever (this is reflected in the lever motion which is sinusoidal to a high degree of accuracy), first-order perturbation theory can naturally be applied to describe the change in the lever characteristics, for instance its resonant frequency shift [5]. However, the success of the perturbative approach may have overwhelmed the fact that for large amplitude operation, the tip dips into a nonlinear surface potential only for a relatively short time so that the nature of the dynamical problem is inherently nonlinear, a “detail” that perhaps has not been fully appreciated.

In this Letter we propose that the damping in (large amplitude) DFM is not mainly a consequence of the action of some dissipation mechanism but rather results from the inaccessibility of some solutions of the microlever equation of motion. This is related to the nonlinearity of the interaction and to the freely oscillating initial conditions imposed in real experiments. It is argued that at some critical tip-surface separation, there is a drastic qualitative change in the analytical resonance curve of the lever (i.e., it becomes multivalued) which is directly related to the emergence of additional damping. Three qualitatively distinct regions of operation are naturally defined within our theory, namely contact, pseudononcontact, and true noncontact. An important aspect of our proposal is that even with a simple model for the interaction force, we can correctly predict orders of magnitude of the experimentally measured “dissipation” and image corrugation, consistently with the microlever frequency shift.

The physical origin of the microlever damping is investigated with the basic equation of motion,

$$\ddot{x} + \omega_0/Q_0\dot{x} + \omega_0^2x = F_d/m + F_i(x + L)/m, \quad (1)$$

where  $\omega_0 = 2\pi f_0 = \sqrt{k/m}$ ,  $Q_0$  are the intrinsic resonant frequency and quality factor of the lever, respectively,

and  $L$  is the mean tip-surface separation.  $F_d(t) = A_d k \times \cos(\omega t)$  is the driving force, and  $F_i$  is the tip-surface interaction force. It is emphasized that the only dissipation mechanism included in Eq. (1) is the intrinsic friction,  $F_i$  being *conservative*. In the following, a simple form for the force  $F_i$  is assumed (LJ type with  $\sigma = 3 \text{ \AA}$ ,  $E_{\text{bond}} = 0.25 \text{ aJ} \approx 1.56 \text{ eV}$ ) that mimics the microscopic interaction between the tip and a rigid surface.  $\omega_0$ ,  $k$ , and  $Q_0$  have been assigned the value  $10^6 \text{ sec}^{-1}$ ,  $26 \text{ N/m}$ , and  $24\,000$ , respectively, so as to reproduce typical experimental conditions. The amplitude at which the lever is to be operated is taken to be  $A_0 = 15\sigma = 4.5 \text{ nm}$ .

We start by finding the steady state solutions of Eq. (1). By Fourier expanding the interaction force  $F_i$  and writing the lever motion as  $x = A \cos(\omega t - \phi)$  [12], the following basic relation can easily be obtained:

$$A = \frac{A_d}{\sqrt{[1 - \omega^2/\omega_0^2 - r(A)]^2 + 1/Q_0^2}}. \quad (2)$$

$r(A)$  is some average of the interaction force over one oscillation period

$$r(A) \equiv \frac{1}{kA^2/2} \frac{1}{2\pi} \int_0^{2\pi} F_i(x + L) A \cos(\theta - \phi) d\theta, \quad (3)$$

with  $\theta \equiv \omega t$ . Equation (2) is, apart from the term  $r(A)$ , what one should expect for a free harmonic oscillator. Analytical resonance curves of the lever can be calculated by inverting Eq. (2),

$$\omega = \omega_0 \sqrt{1 - r(A) \pm \sqrt{\left(\frac{A_d}{A}\right)^2 - \frac{1}{Q_0^2}}}. \quad (4)$$

When the tip is far away from the surface (large  $L$ ), the resonance curve has a Lorentzian shape, as depicted in Fig. 1(a). As the tip-surface separation is reduced, the curve gets continuously deformed and eventually becomes multivalued. Figure 1(a) shows an example of such a behavior for the separation  $L = A_0 + 2\sigma = 5.1 \text{ nm}$ . The current point of view is that the driving frequency at which the response of the lever is maximum, i.e., the resonant frequency, is located at the extremity of the needle edge and corresponds to a frequency shift of  $\Delta f \approx -f_0/2r(A_0)$  [5], as has been pointed out by a few authors [13,14]. Hence the resonant steady state has an amplitude  $A_0$  for a driving amplitude  $A_d = A_0/Q_0$ ; there is no additional damping associated with the surface  $\Delta A_d = 0$ .

It is emphasized that the analytical curves described by Eq. (4) give the amplitude-frequency relation of the mathematically possible steady state solutions of Eq. (1) (as long as the lever motion is well described by a sinusoid). However, other aspects need to be taken into account for a proper description of the actual dynamics of the lever. First, Sasaki *et al.* [13] have demonstrated that the states corresponding to the lower part of the needle edge in Fig. 1(a) are unstable. While stability criteria and Eq. (4) have been implicitly considered as yielding a proper description of the basic problem, in this work

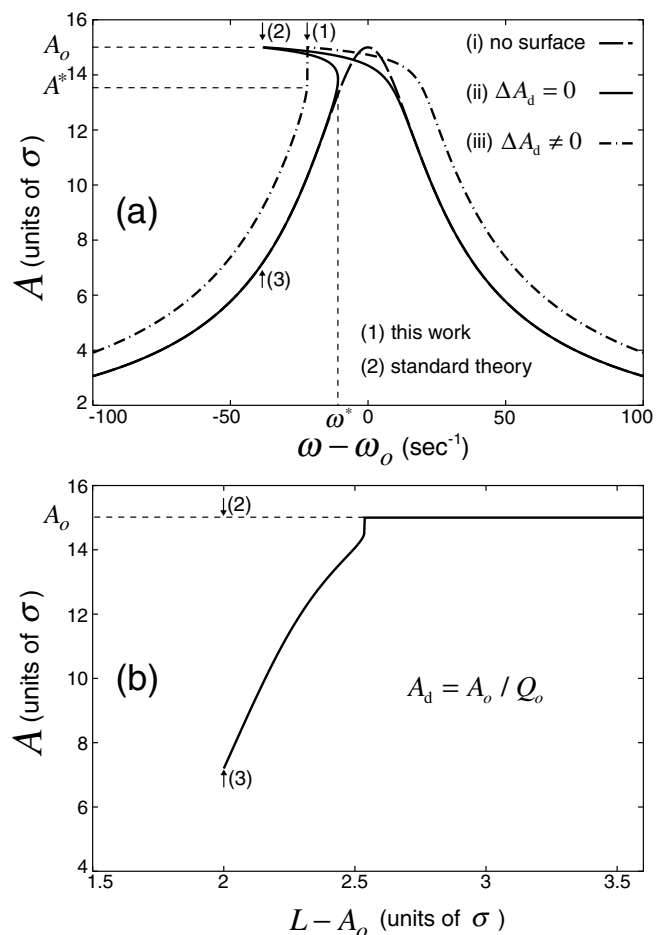


FIG. 1. (a) When the tip is well separated from the surface, the analytical resonance curve is Lorentzian (i) but for  $L = A_0 + 2\sigma$ , it becomes multivalued (ii) with the resonant state located at (2). (b) Lever oscillation amplitude as the mean tip-surface separation is adiabatically reduced from infinity to the separation  $A_0 + 2\sigma$ . The final state reached is not (2) but (3). Note that if the tip is brought more rapidly toward the surface, transient states appear but the final one remains the same. More thorough numerical simulations suggest that under normal operating conditions, the accessible resonance curve is (iii) with resonant state at (1), as shown in (a).

we go a step further. It is well established that the final steady state of a nonlinear dynamical problem may depend on the initial conditions of the system [15]. In the case of DFM, the initial state is not arbitrary; the tip is originally located away from the surface so that it oscillates freely. On the other hand, three parameters are changed dynamically in the course of the approach of the tip to the surface and also during the scanning. These are the separation  $L$ , the driving signal amplitude  $A_d$ , and frequency  $\omega$ . In actual experiments, these parameters are constantly updated by the electronics. The electronics generally consist of a feedback loop that keeps the lever oscillating on its actual resonant frequency, and some regulator which maintains a constant oscillation amplitude. With this setup, constant amplitude experiments are usually performed in the following way: As the tip is approached toward the surface or scanned over the sample

surface, the driving frequency is automatically adjusted to the lever actual resonant frequency until the desired frequency shift is reached. The separation  $L$  and driving amplitude change  $\Delta A_d = A_d - A_0/Q_0$  are then recorded and lead to the so-called topographical and dissipation image of the surface, respectively. Thus, the freely oscillating initial steady state and the systematic way the parameters are modified dynamically may further restrict the lever dynamics in real experiments.

It is therefore of prime importance to investigate the accessibility of the steady state (2) in Fig. 1(a) which has been considered as the resonant one. In Fig. 1(b), Eq. (1) has been numerically integrated starting away from the surface (freely oscillating initial steady state) and modifying the driving frequency according to  $\omega = \omega_0[1 - r(A_0, L)/2]$  during the approach. The driving signal amplitude is fixed to  $A_0/Q_0$ . The final steady state reached in this way is not (2) but the one having a lower amplitude at the same frequency (3). More thorough numerical simulations suggest that the upper side of the needle edge is not accessible if the lever is initially freely oscillating, independently of the way the parameters are brought towards their final value. If the steady state (2) is not accessible under these conditions, the notion of "actual resonance" needs to be revisited. The resonant state would be the one having the largest amplitude. Its frequency  $\omega^*$  coincides with the inflection in the lower branch of the resonance curve but its amplitude is somehow smaller than  $A_0$ ; in constant amplitude experiments, the driving amplitude would have been increased in order to keep it at  $A_0$ . In other words, some damping  $\Delta A_d \neq 0$  exists even if there is no additional dissipation mechanism involved. The accessible resonance curve with the resonant state at  $A_0$  (1) is also plotted in Fig. 1(a).

In order to properly evaluate the resonant frequency shift and the damping  $\Delta A_d$ , one therefore needs to determine the driving signal amplitude  $A_d$ , which ensures that the resonant state has an amplitude  $A_0$ . While the above discussion has been based on a noncontact example, the argument also applies to the contact (repulsive interaction) case as well, as long as the lever motion is still reasonably described by a sinusoid [12].  $A_d$  can be obtained by solving the following 2 (nonlinear) master equations ( $A^*$  is the other unknown):

$$\pm \sqrt{\left(\frac{A_{d_r}}{A^*}\right)^2 - \frac{1}{Q_0^2}} \Delta(A^*) = \left(\frac{A_{d_r}}{A^*}\right)^2, \quad (5)$$

$$-r(A_0) \pm \sqrt{\left(\frac{A_{d_r}}{A_0}\right)^2 - \frac{1}{Q_0^2}} = -r(A^*) \mp \sqrt{\left(\frac{A_{d_r}}{A^*}\right)^2 - \frac{1}{Q_0^2}}, \quad (6)$$

with  $\Delta(A^*) \equiv -r(A^*) + g(A^*)$ .  $g(A)$  is defined as

$$g(A) \equiv \frac{1}{kA^2/2} \frac{1}{2\pi} \int_0^{2\pi} \frac{dF_i(x+L)}{dx} \times A^2 \cos^2(\theta - \phi) d\theta, \quad (7)$$

and  $A^*$  is illustrated in Fig. 1(a). Equation (5) is used to determine  $\omega^*$  and Eq. (6) imposes the condition that the resonant state must have an amplitude  $A_0$ .  $\Delta A_d = A_d - A_0/Q_0$  is thus a function of  $L$  implicitly through the quantity  $r(A)$  and  $g(A)$ . Note that Eq. (5) is valid for  $A_{d_r} > A^*/Q_0$ , else  $A_d = A_0/Q_0$ . Also,  $\Delta(A^*)$  and therefore  $\Delta A_d$  vanish for very small amplitude or linear interaction.

The frequency shift  $\Delta f$  [Eq. (4)] and apparent energy dissipation associated with the damping  $\Delta E = kA_0/2\Delta A_d$ , are calculated by solving Eqs. (5) and (6) numerically and are shown in Fig. 2. The upper and lower signs in Eqs. (4)–(6) are used to calculate the noncontact and contact branch, respectively, and a close inspection of the resonance curves around  $L - A_0 \approx \sigma$  reveals that there is a small region where no curve has its resonant state with amplitude  $A_0$ . The noncontact branch can be further divided into two regions, namely pseudo and true noncontact. They differ from each other in that

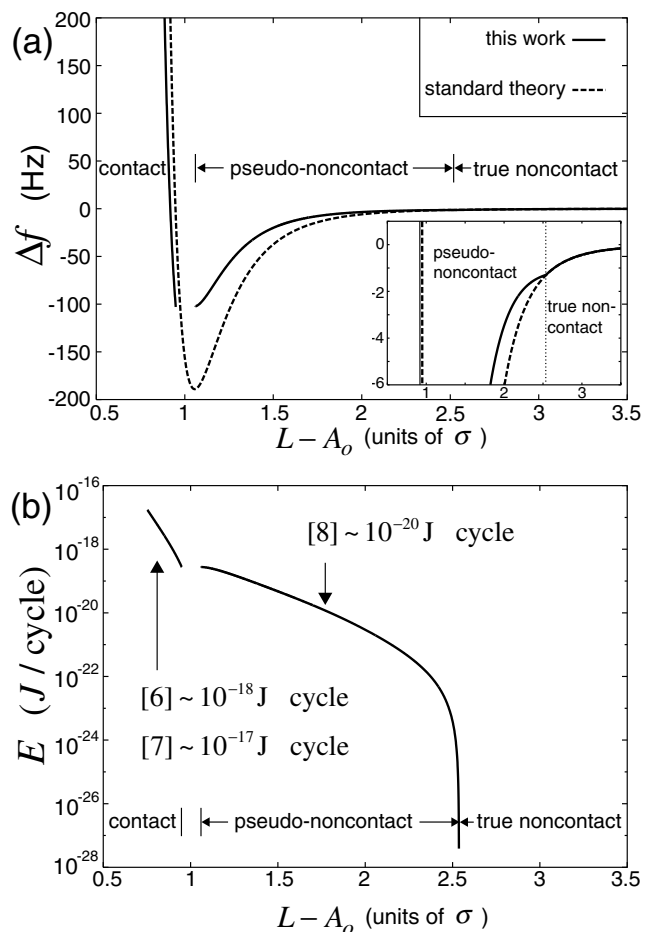


FIG. 2. (a) Frequency shift, and (b) apparent energy dissipation obtained from Eqs. (5) and (6) as a function of the distance of closest approach. Three regions of operation can be seen: contact, pseudononcontact, and true noncontact. In (a), the frequency shift is also compared with the standard theory,  $\Delta f = -f_0/2r(A_0)$ . The two curves are identical in the true noncontact regime. (b) Order of magnitude compares well with various experiments.

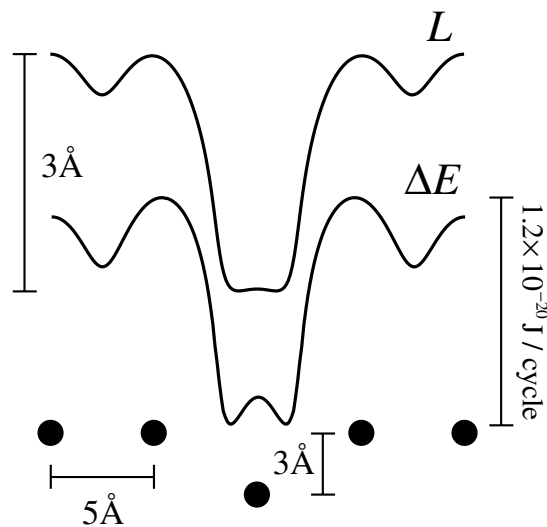


FIG. 3. Corrugation of the quantity  $L$  and  $\Delta E$  obtained by scanning the tip over a one-dimensional surface model with a defect at constant frequency shift  $\Delta f = -80$  Hz. The corrugations agree well with experiments [8].

the analytical resonance curve in the pseudo-noncontact region is multivalued as opposed to single valued in the true noncontact region. The critical separation associated with the onset of the multivalued behavior (where  $A^*$  is no longer equal to  $A_0$ ) is an implicit function of the interaction force through the quantity  $r(A)$  and  $g(A)$ . It corresponds to the maximum separation  $L$  where Eq. (5) admits a solution.

It is remarkable that even with a very simple form for the interaction force, we are able to reproduce correctly orders of magnitude of experimentally inferred energy dissipation obtained in very different conditions and samples [Fig. 2(b)].

For large amplitude operations, the damping mechanism described in this work is likely to be a dominant effect. The possibility of achieving true atomic resolution via this mechanism is briefly examined on a one-dimensional surface model with a defect. Figure 3 shows the result of a scan at constant frequency shift  $\Delta f = -80$  Hz for both the quantity  $L$  and  $\Delta E$ . Note the enhanced and slightly shifted damping over the atoms next to the defect. These features and the calculated corrugations agree well with experiments [8].

In summary, it is argued that the additional damping effects in DFM do not mainly result from energy dissipation,

but arise because not all solutions of Eq. (1) are accessible. We are able to reproduce orders of magnitude of experimentally measured “dissipation” in various conditions of operation and their image corrugation. The damping is found to be related to the multivalued nature of the analytical resonance curve. We have obtained some numerical indications that the proposal made here is consistent with a phase locked at  $90^\circ$ . More theoretical work is, however, necessary in order to clearly establish how such a relationship may arise.

This work was supported in part by a Grant-in-Aid on Priority Areas from the Ministry of Education, Science and Culture, Japan. The first author acknowledges support from the Ministry of Education of Japan. The authors would like to thank N. Sasaki and S. Nakanishi for useful discussions.

- [1] T. R. Albrecht, P. Grütter, D. Horne, and D. Rugar, *J. Appl. Phys.* **69**, 668 (1991).
- [2] F. J. Giessibl, *Science* **267**, 68 (1995).
- [3] S. Kitamura and M. Iwatsuki, *Jpn. J. Appl. Phys.* **34**, L145 (1995).
- [4] H. Ueyama, M. Ohta, Y. Sugawara, and S. Morita, *Jpn. J. Appl. Phys.* **34**, L1086 (1995).
- [5] F. J. Giessibl, *Phys. Rev. B* **56**, 16010 (1997).
- [6] U. Dürig, H. R. Steinauer, and N. Blanc, *J. Appl. Phys.* **82**, 3641 (1997).
- [7] B. Anczykowski, B. Gotsmann, H. Fuchs, J. P. Cleveland, and V. B. Elings, *Appl. Surf. Sci.* **140**, 376 (1999).
- [8] R. Bennowitz, A. S. Foster, L. N. Kantorovich, M. Bammerlin, Ch. Loppacher, S. Schär, M. Guggisberg, E. Meyer, and A. L. Shluger, *Phys. Rev. B* **62**, 2074 (2000).
- [9] R. Bennowitz, M. Bammerlin, M. Guggisberg, C. Loppacher, A. Baratoff, E. Meyer, and H.-J. Güntherodt, *Surf. Sci.* **438**, 289 (1999).
- [10] M. Gauthier and M. Tsukada, *Phys. Rev. B* **60**, 11716 (1999).
- [11] A. Abdurixit, T. Bonner, A. Baratoff, and E. Meyer, *Appl. Surf. Sci.* **157**, 355 (2000).
- [12] Fourier analysis can be used to demonstrate that the higher harmonic corrections are small for most cases of interest (even when the interaction becomes repulsive).
- [13] N. Sasaki and M. Tsukada, *Appl. Surf. Sci.* **140**, 339 (1999).
- [14] J. P. Aimé, R. Boisgard, L. Nony, and G. Couturier, *Phys. Rev. Lett.* **82**, 3388 (1999).
- [15] J. Guckenheimer and P. Holmes, *Nonlinear Oscillations, Dynamical Systems, and Bifurcations of Vector Field* (Springer-Verlag, New York, 1983).